Electronic Supplementary Material (ESI) for Physical Chemistry Chemical Physics.

Supplementary Material

Superconducting boron allotrope featuring pentagonal bipyramid at ambient pressure

Shuai Han[1,3], Yunxian Liu[1,2*], Chao Wang[1,2], Wencai Yi[1,2], Xin Chen[1,2], Yongsheng Zhang[1,2] and Xiaobing Liu[1,2*]

[1]*Laboratory of High Pressure Physics and Material Science, School of Physics and Physical Engineering, Qufu Normal University, Qufu, Shandong Province, 273165, China*

[2]*Advanced Research Institute of Multidisciplinary Sciences, Qufu Normal University, Qufu, Shandong Province, 273165, China*

[3]*Center for High Pressure Science and Technology Advanced Research, Beijing, 100094, China*

Email: yunxianliu@qfnu.edu.cn; xiaobing.phy@qfnu.edu.cn

Supplemental figures

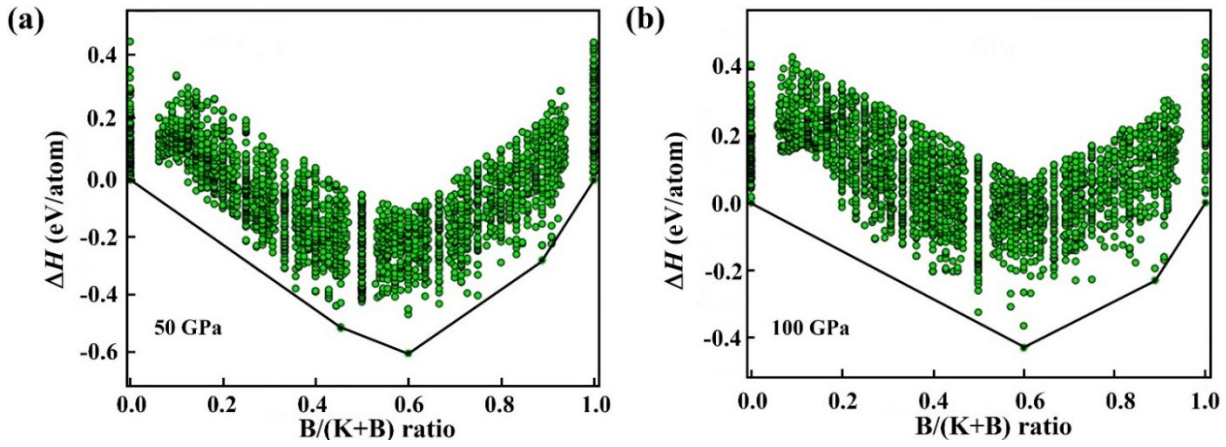

Figure S1. Variable composition structural searches at fixed pressure of 50 and 100 GPa for the K–B system. We consider the maximum composition is K:B = 1:10 in the B-rich region.

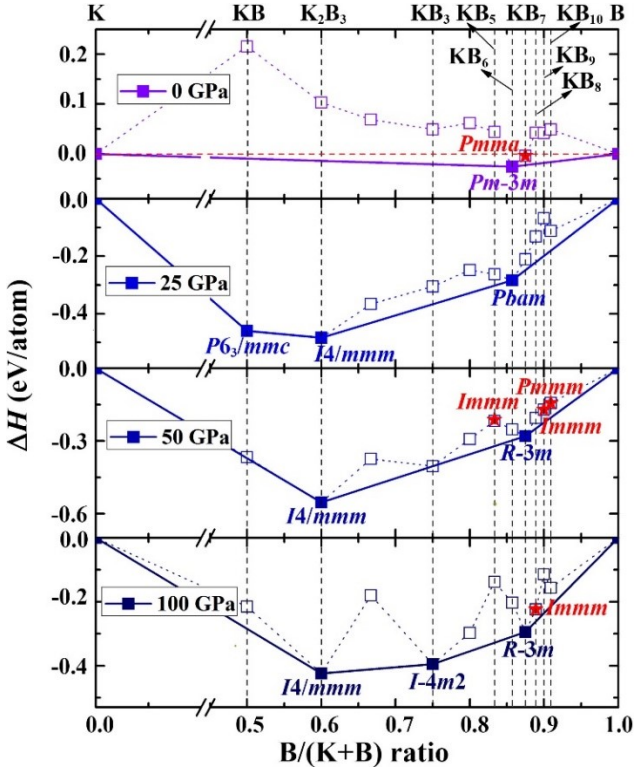

Figure S2. Formation enthalpies of predicted K–B compounds with various composition ratios at 0 GPa, 25 GPa, 50 GPa and 100 GPa. The stable configurations on the convex hull are marked by solid symbols, while unstable configurations are marked by open symbols. The red stars near convex hull represent metastable phases of K–B compounds with higher enthalpy. Four new B-rich stoichiometries (i.e., KB, K_2B_3, KB_3, KB_7) emerge on the convex hull at high pressure, and the low-pressure *Pm*-3*m* KB_6 phase[1, 2] is well reproduced, indicating our adopted structure searching method apply to the K–B system.

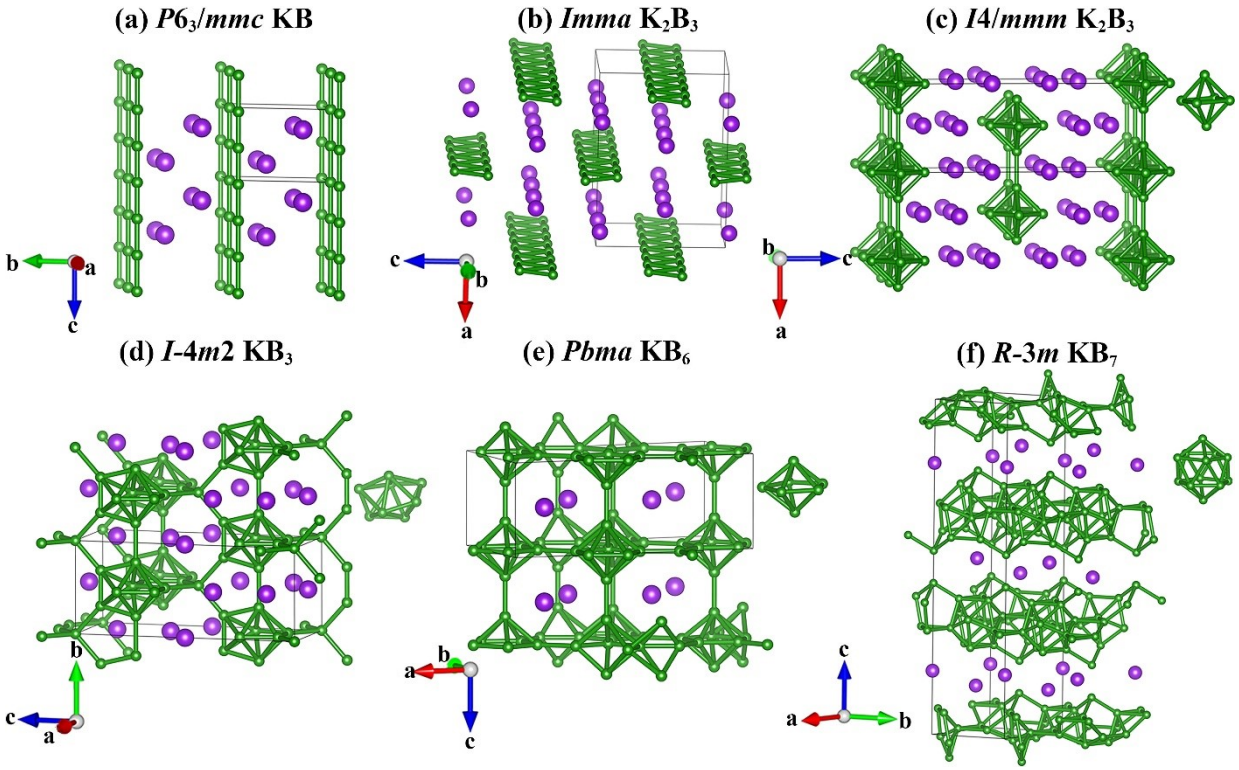

Figure S3. The predicted new stable structures in the K–B system. (a) *P*6$_3$/*mmc* KB, (b) *Imma* K_2B_3, (c) *I*4/*mmm* K_2B_3, (d) *I*-4*m*2 KB_3, (e) *Pbma* KB_6 and (f) *R*-3*m* KB_7.

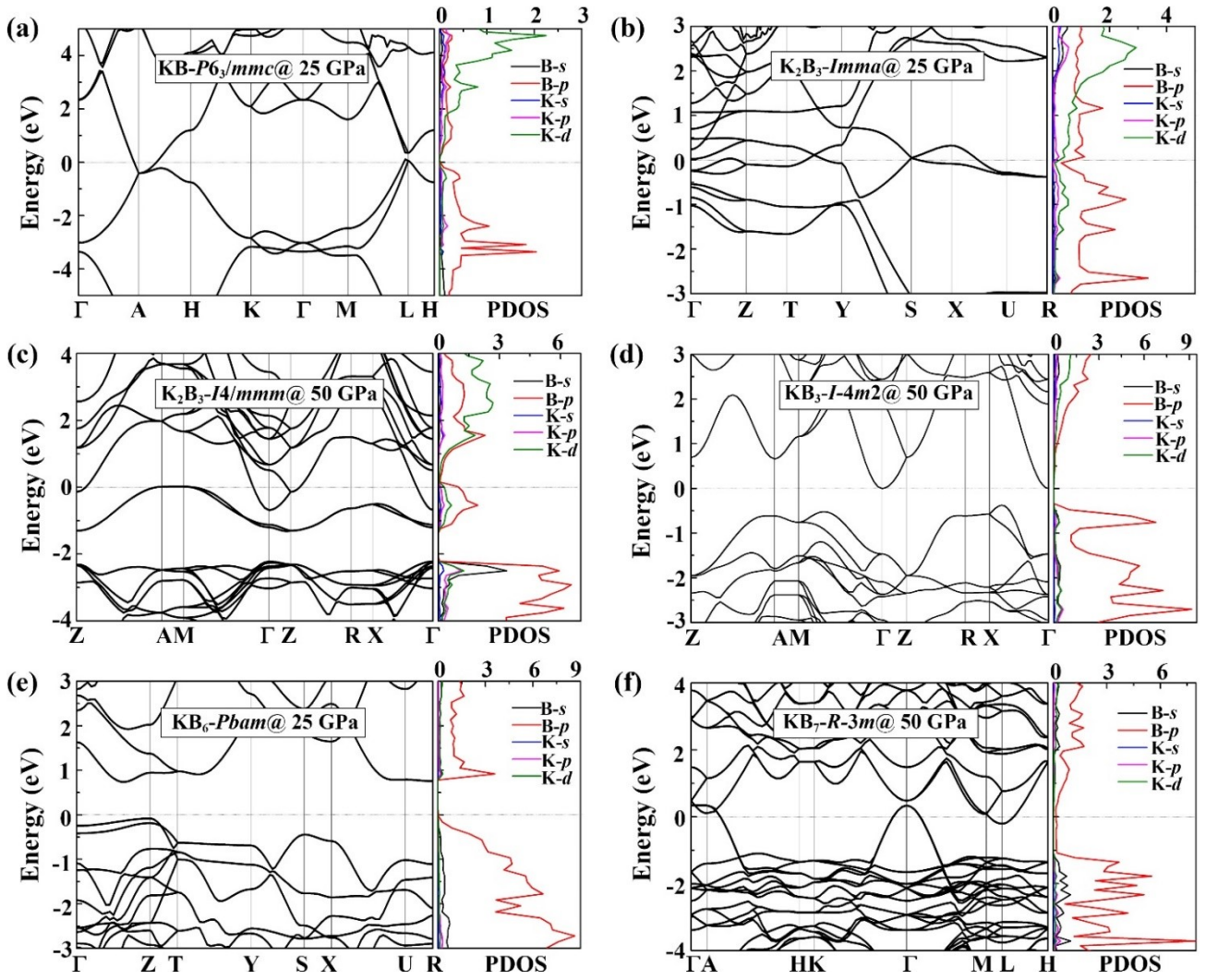

Figure S4. Electronic band structures and corresponding projected density of states (PDOS) of the predicted K–B compounds. (a) $P6_3/mmc$ KB at 25 GPa. (b) *Imma* K_2B_3 at 25 GPa. (c) $I4/mmm$ K_2B_3 at 50 GPa. (d) $I\text{-}4m2$ KB_3 at 50 GPa. (e) *Pbma* KB_6 at 25 GPa. (f) $R\text{-}3m$ KB_7 at 50 GPa.

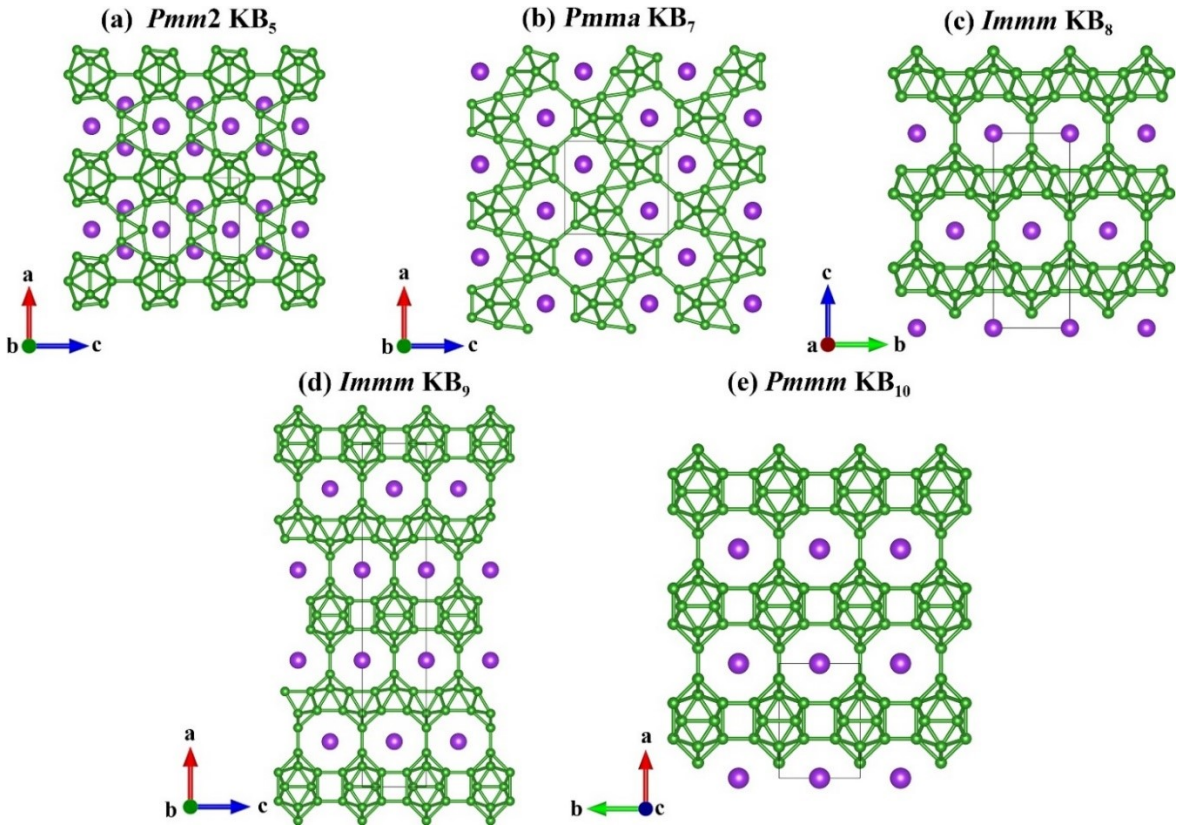

Figure S5. The crystal structures of (a) *Pmm*2 KB_5 at 50 GPa, (b) *Pmma* KB_7 at 0 GPa, (c) *Immm* KB_8 at 100 GPa, (d) *Immm* KB_9 at 50 GPa and (e) *Pmmm* KB_{10} at 50 GPa.

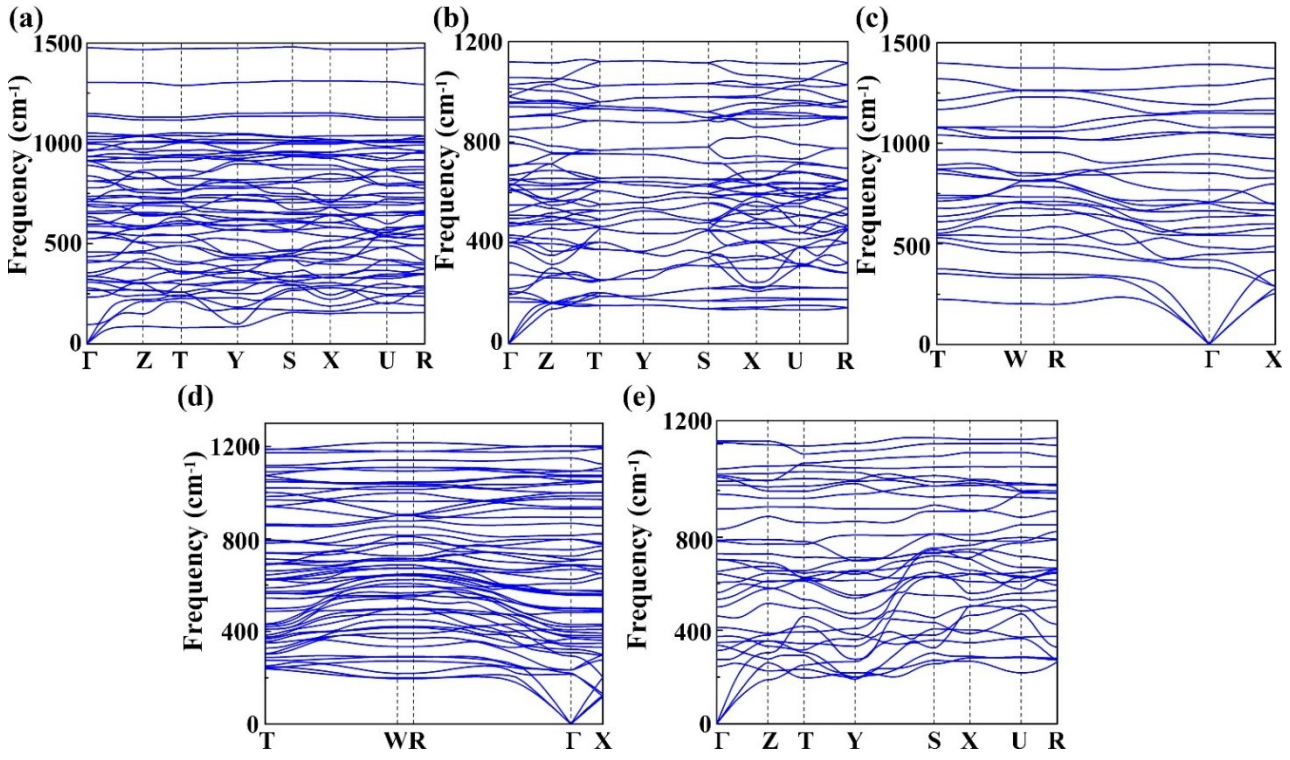

Figure S6. Phonon dispersion curves for (a) *Pmm*2 KB_5, (b) *Pmma* KB_7, (c) *Immm* KB_8, (d) *Immm* KB_9 and (e) *Pmmm* KB_{10} at selected pressures.

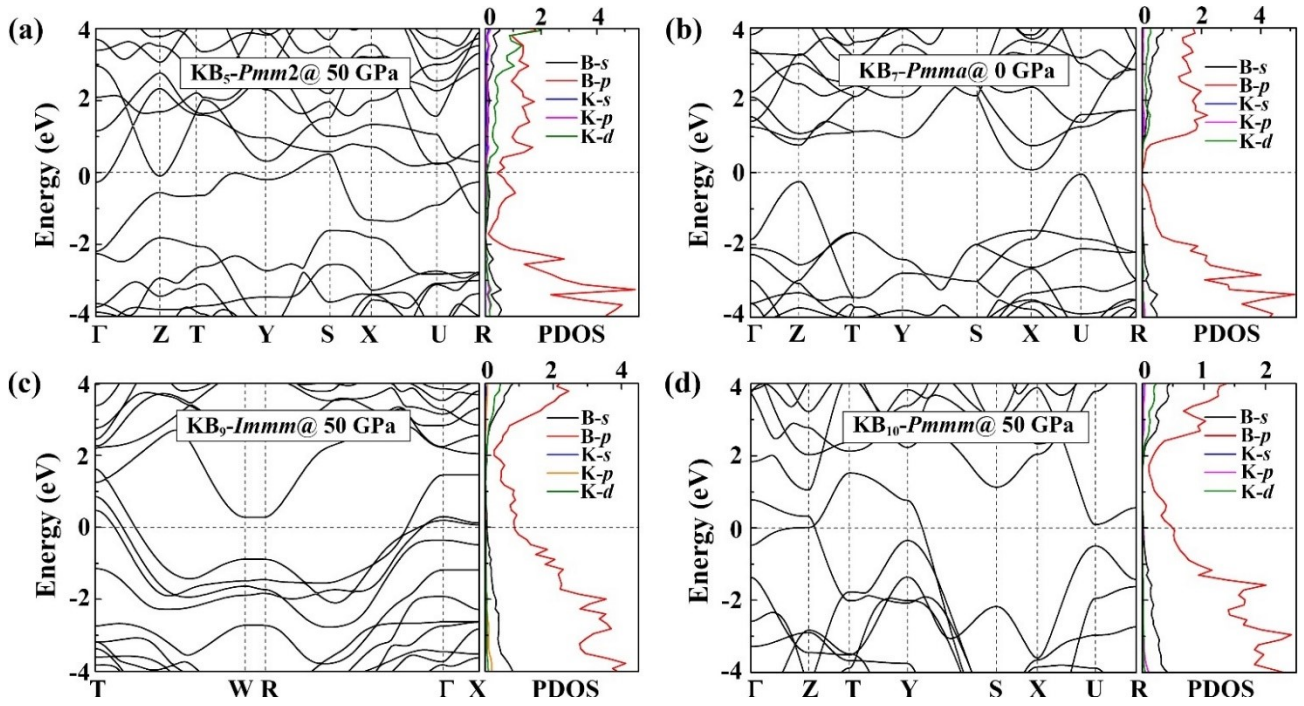

Figure S7. Electronic band structures and corresponding projected density of states (PDOS) of (a) *Pmm*2 KB_5, (b) *Pmma* KB_7, (c) *Immm* KB_9 and (d) *Pmmm* KB_{10} at selected pressures.

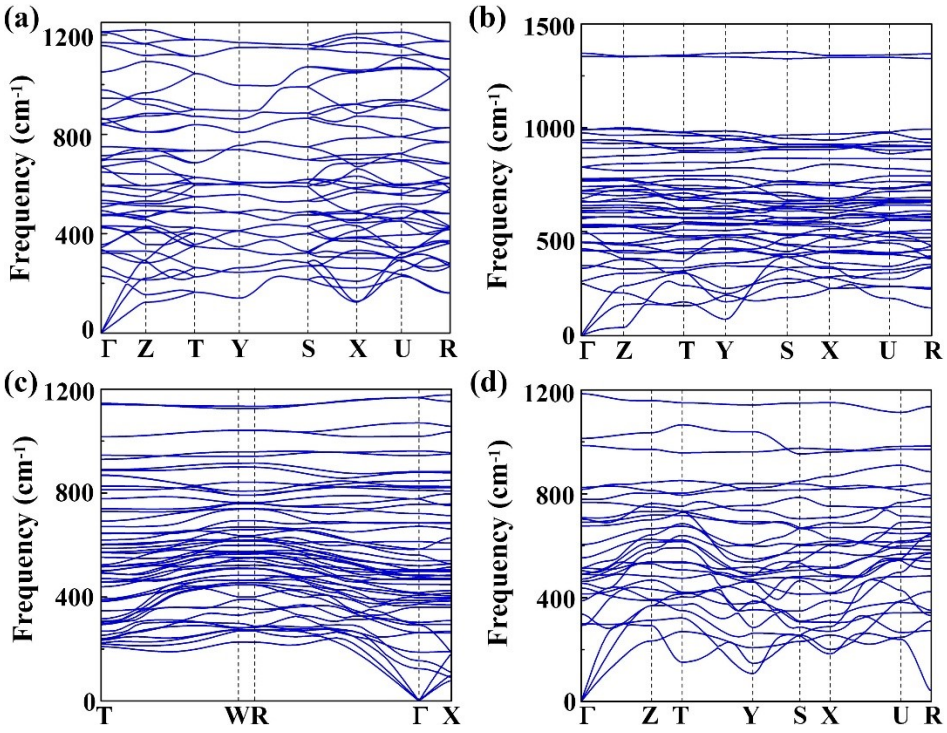

Figure S8. Phonon dispersion curves for (a) *o*-B_{14}, (b) *o*-B_{15}, (c) *o*-B_{36} and (d) *o*-B_{10} at 1 atm.

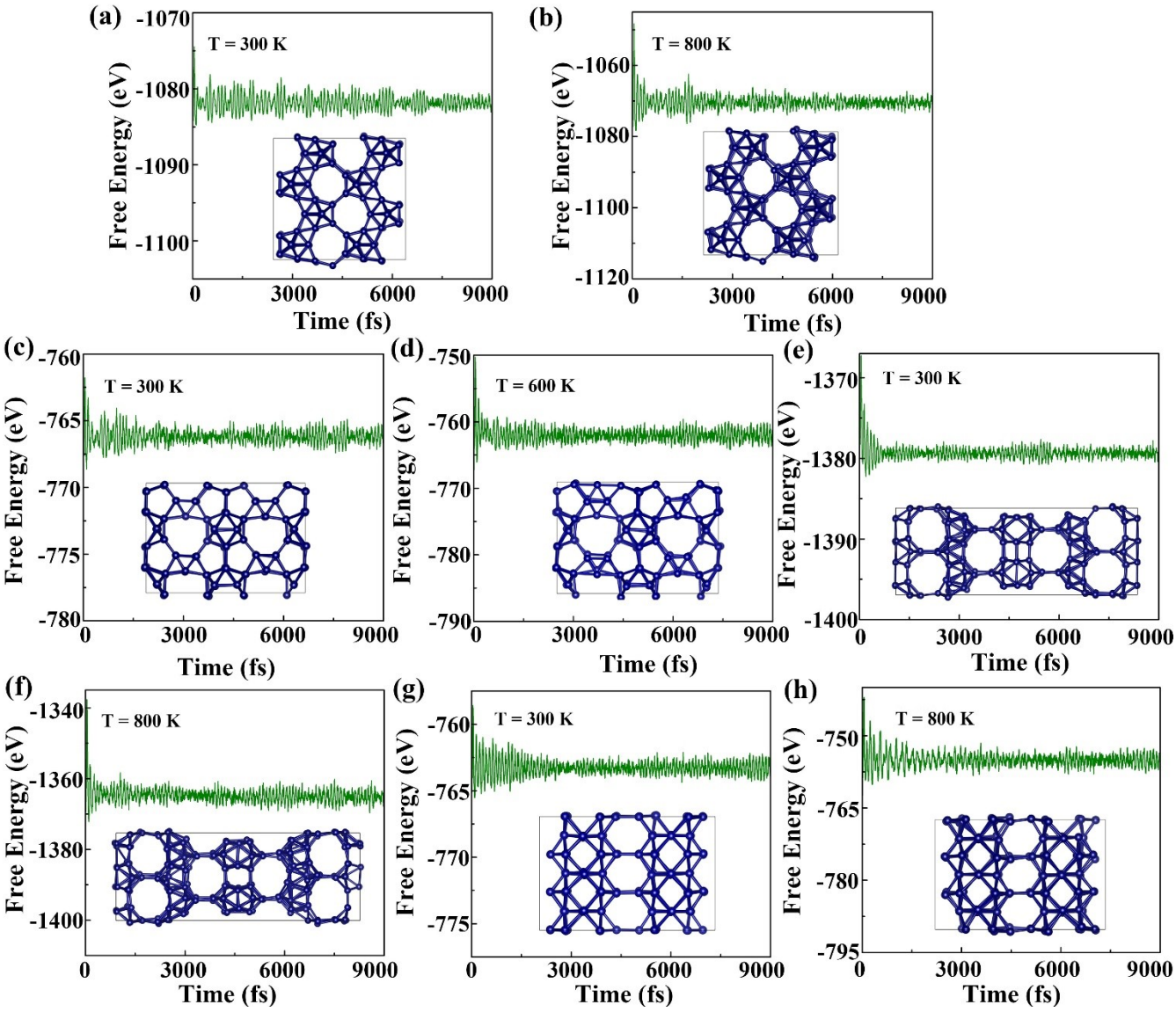

Figure S9. The free energy fluctuation of boron allotropes supercell varies with the time step of MD simulations for *o*-B_{14} at (a) 300 K and (b) 800 K, *o*-B_{15} at (c) 300 K and (d) 600 K, *o*-B_{36} at (e) 300 K and (f) 800 K, and *o*-B_{10} at (g) 300 K and (h) 800 K, showing the snapshot of the simulated system.

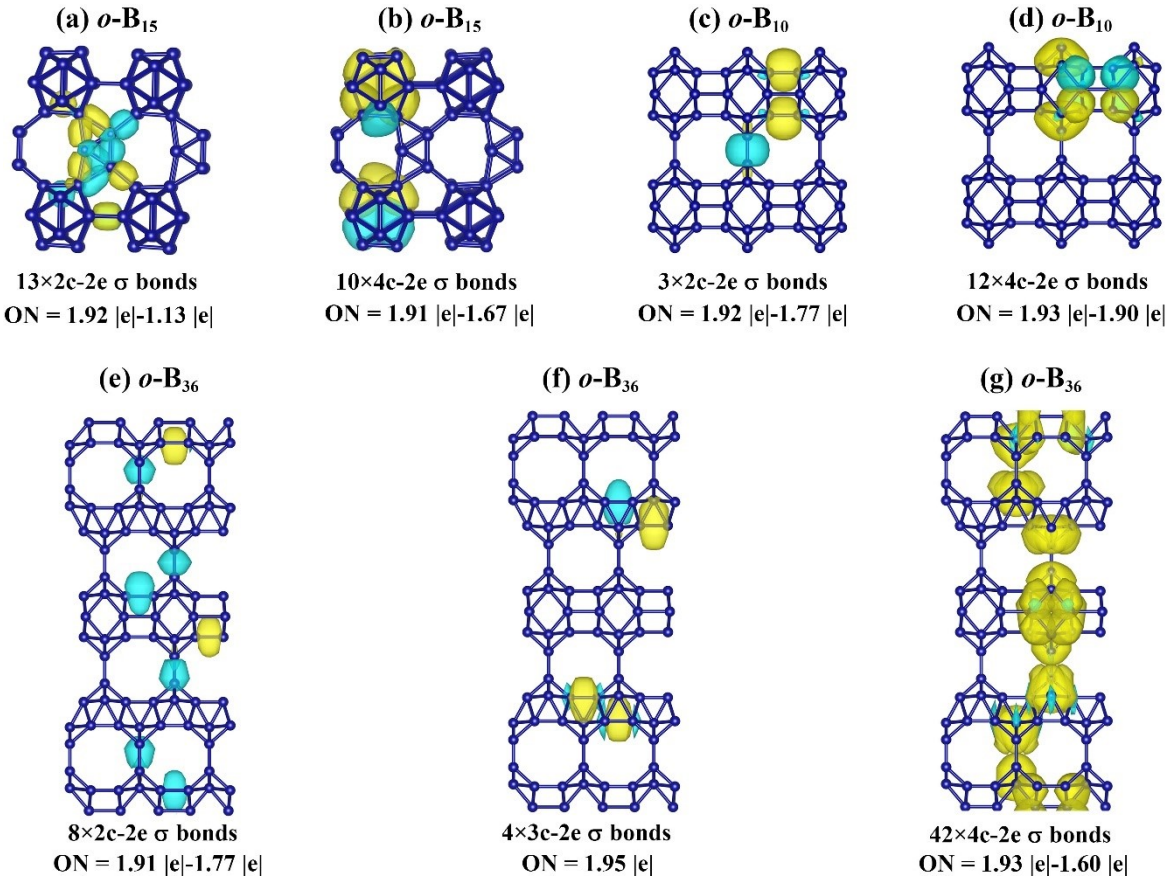

Figure S10. The SSAdNDP chemical bonding analysis of *o*-B_{15}, *o*-B_{10} and *o*-B_{36} with the occupation number (ON). For *o*-B_{15}, total 23 bonds are shown, including (a) thirteen 2c–2e σ bonds and (b) teen 4c–2e σ bonds. For *o*-B_{10}, total 15 bonds are shown, including (c) three 2c–2e σ bonds and (d) twelve 4c–2e σ bonds. For *o*-B_{36}, total 54 bonds are shown, including (e) eight 2c–2e σ bonds, (f) four 2c–2e σ bonds and (g) forty-two 4c–2e σ bonds.

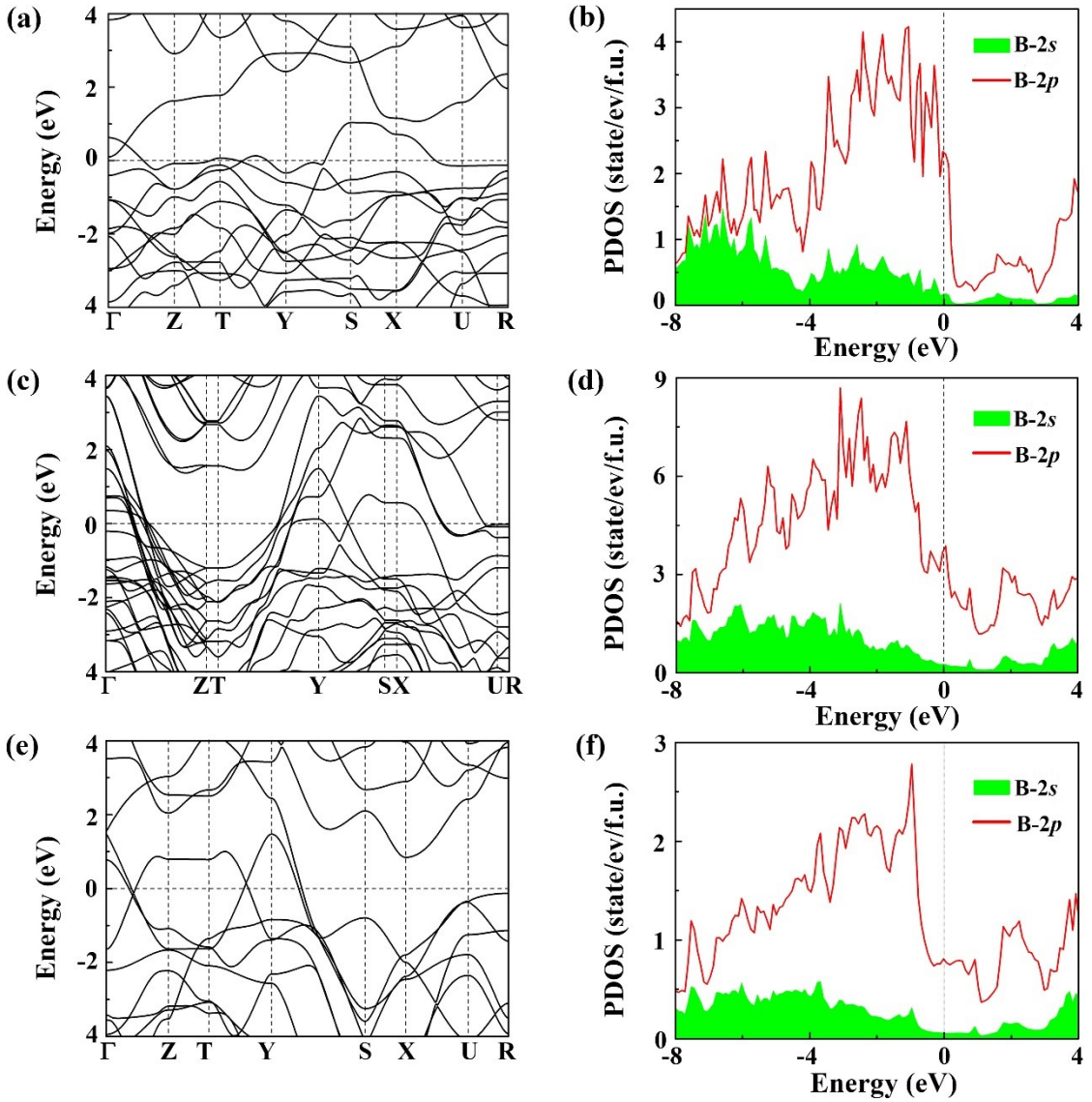

Figure S11. Electronic band structures for (a) *o*-B_{15}, (c) *o*-B_{36} and (e) *o*-B_{10} at 1 atm, corresponding projected density of states (PDOS) for (b) *o*-B_{15}, (d) *o*-B_{36} and (f) *o*-B_{10} at 1 atm.

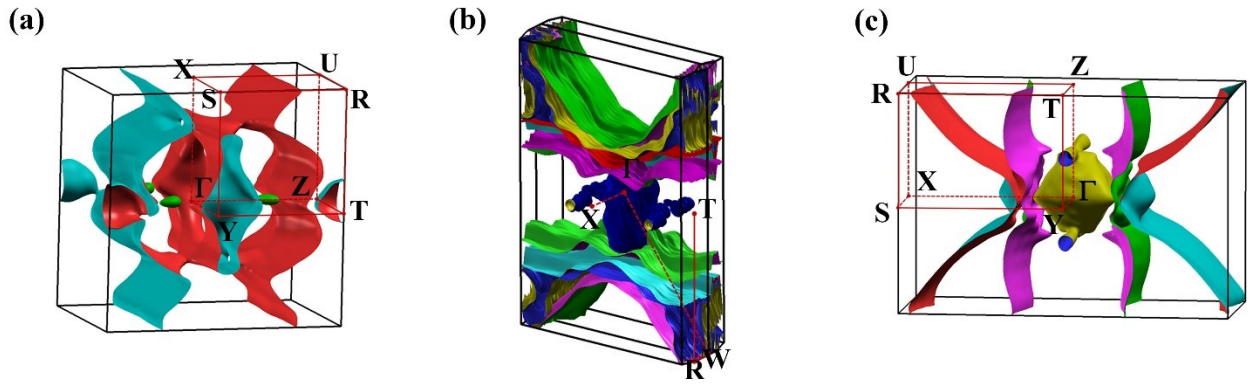

Figure S12. The Fermi surface for (a) *o*-B_{15}, (b) *o*-B_{36} and (c) *o*-B_{10} at 1 atm.

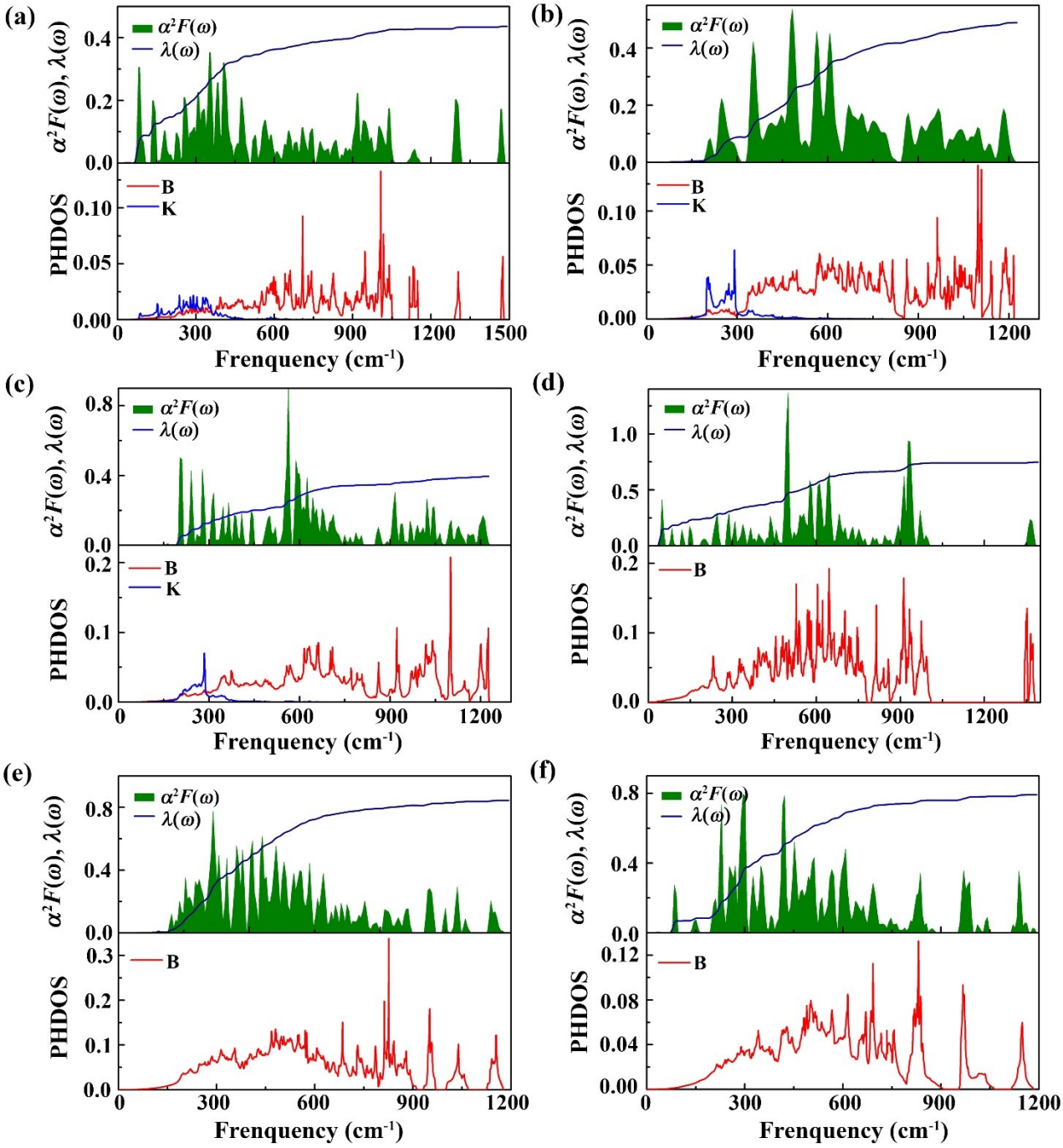

Figure S13. The Eliashberg phonon spectral function $\alpha^2F(\omega)$ together with the integrated electron–phonon spectral coupling $\lambda(\omega)$ and the projected phonon density of state (PHDOS) of (a) *Pmm*2 KB_5, (b) *Immm* KB_9, (c) *Pmmm* KB_{10} at 50 GPa and (d) *o*-B_{15}, (e) *o*-B_{36}, (f) *o*-B_{10} at 0 GPa.

Supplemental table

Table S1. Structural information of the predicted stable K–B phases and metastable K–B phases.

Structure	Pressure	Lattice Parameters (Å, °)	Atomic positions
*P*6$_3$/*mmc* KB	25 GPa	$a = b = 4.6607$	B (2a) (0.00000, 0.00000, 0.00000)
		$c = 3.0280$	K (2d) (0.33333, 0.66667, 0.75000)
		$\alpha = \beta = \gamma = 90$	
Imma K_2B_3	10 GPa	$a = 8.7022$	B1 (8h) (0.00000, 1.07859, 0.62691)
		$b = 5.0299$	B2 (4e) (0.00000, 0.75000, 0.62566)
		$c = 6.3197$	K (8i) (0.18473, 0.75000, 1.00069)
		$\alpha = \beta = \gamma = 90$	
*I*4/*mmm* K_2B_3	50 GPa	$a = b = 4.1508$	B1 (4e) (0.00000, 0.00000, −0.89298)
		$c = 11.5340$	B2 (8i) (0.00000, −0.29209, 0.00000)
		$\alpha = \beta = \gamma = 90$	K1 (4e) (0.00000, 0.00000, −0.61752)
			K2 (4d) (0.00000, −0.50000, −0.25000)
I-4*m*2 KB_3	100 GPa	$a = b = 4.1143$	B1 (8i) (−0.50000, 0.18979, 0.38442)
		$c = 10.0127$	B2 (8i) (−0.50000, 0.28738, 0.22449)
		$\alpha = \beta = \gamma = 90$	B3 (2a) (0.00000, 0.00000, 0.00000)
			K1 (4f) (0.00000, 0.50000, 0.37218)
			K2 (2b) (0.00000, 0.00000, 0.50000)
Pbam KB_6	25 GPa	$a = 10.7009$	B1 (8i) (0.41214, 0.86434, 0.71402)
		$b = 5.5374$	B2 (4g) (0.45085, 0.11586, 0.00000)
		$c = 3.9879$	B3 (4g) (0.19346, 0.51333, 0.00000)
		$\alpha = \beta = \gamma = 90$	B4 (4g) (0.53367, 0.36387, 0.00000)
			B5 (4g) (0.31489, 0.70955, 0.00000)
			K (4h) (0.35032, 0.36849, 0.50000)
R-3*m* KB_7	50 GPa	$a = b = 4.4233$	B1 (18h) (0.13420, −0.13420, 0.68299)
		$c = 19.5621$	B2 (6c) (0.00000, 0.00000, 0.45161)
		$\alpha = \beta = 90$	B3 (6c) (0.00000, 0.00000, 0.81006)
		$\gamma = 120$	K (18h) (−0.395488, −0.19774, 0.59631)
*Pmm*2 KB_5	50 GPa	$a = 6.6311$	B1 (4i) (0.12852, 0.68962, −0.14935)
		$b = 4.5941$	B2 (1c) (0.50000, 0.00000, −0.39382)
		$c = 4.4626$	B3 (2e) (0.21362, 0.00000, −0.95283)
		$\alpha = \beta = \gamma = 90$	B4 (2e) (0.61688, 0.00000, −0.69856)

			B5 (2e) (0.76123, 0.00000, −0.33459)
			B6 (2g) (1.00000, 0.18235, −0.83710)
			B7 (2g) (1.00000, 0.81903, −0.45852)
			K1 (1d) (0.50000, 0.50000, −0.12522)
			K2 (2f) (0.70659, 0.50000, −0.64037)
Pmma KB_7	0 GPa	a = 5.7502	B1 (4j) (0.52128, 0.50000, 0.64266)
		b = 4.2472	B2 (4j) (0.60090, 0.50000, 0.89548)
		c = 6.4126	B3 (4k) (0.75000, 0.78813, 0.72193)
		$\alpha = \beta = \gamma = 90$	B4 (2f) (0.25000, 0.50000, 0.51482)
			K (2e) (0.25000, 0.00000, 0.81764)
Immm KB_9	50 GPa	a = 22.7841	B1 (4e) (0.09862, −1.00000, 0.00000)
		b = 4.2593	B2 (8n) (0.27751, −1.20084, −0.50000)
		c = 2.7619	B3 (4f) (−0.06009, −1.00000, −0.50000)
		$\alpha = \beta = \gamma = 90$	B4 (4f) (0.21332, −1.00000, −0.50000)
			B5 (4h) (0.00000, −0.79470, −0.50000)
			B6 (8n) (−0.04174, −0.30275, 0.00000)
			B7 (4e) (0.32808, −1.50000, −0.50000)
			K (4e) (0.36839, −1.00000, 0.00000)
Pmmm KB_{10}	50 GPa	a = 6.0909	B1 (4x) (0.34514, 0.50000, 0.30311)
		b = 2.7938	B2 (2s) (0.50000, 0.00000, 0.20361)
		c = 4.3060	B3 (2k) (0.13479, 0.50000, 0.00000)
		$\alpha = \beta = \gamma = 90$	B4 (2i) (0.27525, 0.00000, 0.00000)
			K (1c) (0.00000, 0.00000, 0.50000)

Table S2. Bader atomic charges of the predicted metastable K–B phases.

Structure	Pressure (GPa)	Atom	Charge (e)
*Pmm*2 KB_5	50	B1	−0.164
		B2	0.198
		B3	0.244
		B4	−0.839
		B5	0.079
		B6	−0.064
		B7	−0.107
		K1	1.652
		K2	1.589
Pmma KB_7	0	B1	−0.054
		B2	−0.094
		B3	0.077
		B4	−0.610
		K	1.752
Immm KB_9	50	B1	−0.058
		B2	−0.140
		B3	−0.152
		B4	0.047
		B5	−0.610
		B6	0.257
		B7	−0.104
		K	1.643
Pmmm KB_{10}	50	B1	−0.054
		B2	−0.094
		B3	0.077
		B4	−0.610
		K	1.752

Table S3. Structural information for the new B allotropes at 1 atm.

Structure	Lattice Parameters (Å, °)	Atomic positions
o-B_{15}	a = 6.6403	B1 (4i) (0.13930, 0.68483, 0.85095)
	b = 4.6931	B2 (1c) (0.50000, 0.00000, 0.60154)
	c = 4.5870	B3 (2e) (0.22088, 0.00000, 0.04310)
	$\alpha = \beta = \gamma = 90$	B4 (2e) (0.62374, 0.00000, 0.31868)
		B5 (2e) (0.76704, 0.00000, 0.66327)
		B6 (2g) (0.00000, 0.19565, 0.16035)
		B7 (2g) (0.00000, 0.79972, 0.53502)
o-B_{14}	a = 5.6970	B1 (4x) (0.52123, 0.50000, 0.93796)
	b = 4.0479	B2 (4j) (0.55975, 0.50000, 0.89991)
	c = 6.2042	B3 (4k) (0.75000, 0.79171, 0.72973)
	$\alpha = \beta = \gamma = 90$	B4 (2f) (0.25000, 0.50000, 0.52367)
o-B_{36}	a = 23.8183	B1 (4e) (−0.10179, 0.00000, 0.00000)
	b = 4.2733	B2 (4e) (−0.82793, 0.00000, 0.00000)
	c = 2.8125	B3 (8n) (−0.28016, 0.19841, 0.50000)
	$\alpha = \beta = \gamma = 90$	B4 (8n) (−0.44748, −0.20083, 0.50000)
		B5 (4f) (−0.44172, −0.50000, 0.00000)
		B6 (4f) (−0.21494, 0.00000, 0.50000)
		B7 (4h) (0.00000, −0.27352, 0.50000)
o-B_{10}	a = 6.5336	B1 (4x) (0.30695, 0.50000, 0.29846)
	b = 2.8213	B2 (2s) (0.50000, 0.00000, 0.27392)
	c = 4.2261	B3 (2k) (0.12775, 0.50000, 0.00000)
	$\alpha = \beta = \gamma = 90$	B4 (2i) (0.28654, 0.00000, 0.00000)

Table S4. Gibbs free energy differences of *o*-B_{15}, *o*-B_{14}, *o*-B_{36} and *o*-B_{10} with respect to *α*-B_{12}[3] at 1 atm.

	$G(o\text{-}B_{15}) - G(\alpha\text{-}B_{12})$	$G(o\text{-}B_{14}) - G(\alpha\text{-}B_{12})$	$G(o\text{-}B_{36}) - G(\alpha\text{-}B_{12})$	$G(o\text{-}B_{10}) - G(\alpha\text{-}B_{12})$
Δ*G* (eV/atom)	0.276	0.232	0.292	0.322

Table S5. Elastic stiffness constants C_{ij} (GPa), bulk modulus *B* (GPa), shear modulus *G* (GPa), Pugh criterion (*B*/*G*), Poisson's ratio *v* and Vickers hardness H_v (GPa) for B allotropes.

	C_{11}	C_{22}	C_{33}	C_{44}	C_{55}	C_{66}	C_{12}	C_{13}	C_{23}	*G*	*B*	*v*	*B/G*	H_v
o-B_{15}	278	267	421	15	120	8	47	89	25	53	140	0.33	2.65	3.48
o-B_{14}	414	238	336	41	194	33	32	117	25	87	141	0.24	1.62	12.38
o-B_{36}	453	499	430	47	134	80	107	80	21	114	199	0.26	1.75	13.53
o-B_{10}	445	506	436	80	165	63	87	115	239	125	204	0.25	1.64	15.92

In the orthorhombic boron allotropes structures, the nine independent elastic constants meet the following mechanical stability criteria: $C_{11} > 0$, $C_{22} > 0$, $C_{33} > 0$, $C_{44} > 0$, $C_{55} > 0$, $C_{66} > 0$, $[C_{11} + C_{22} + C_{33} + 2(C_{12} + C_{13} + C_{23})] > 0$, $(C_{11} + C_{22} - 2C_{12}) > 0$, $(C_{11} + C_{33} - 2C_{13}) > 0$, $(C_{22} + C_{33} - 2C_{23}) > 0$.[4]

Table S6. The electron–phonon coupling (EPC) constant λ, the logarithmic average phonon frequency ω_{log}, and the electronic DOS at the Fermi level $N(\varepsilon_f)$ and superconducting transition temperature (T_c) for K–B structures and B allotropes at ambient pressure.

Structure	P(GPa)	λ	ω_{log}(K)	$N(\varepsilon_f)$	T_c(K)μ^*=0.1
P6_3/*mmc* KB	50	0.62	88.73	3.03	2.27
*I*4/*mmm* K_2B_3	25	0.11	542.86	4.48	0
Pm-3*m* KB_6	0	0.54	790.63	11.05	12.41
R-3m KB_7	50	0.24	910.87	1.93	0.03
*Pmm*2 KB_5	50	0.44	398.83	10.53	2.66
Immm KB_9	50	0.49	703.984	10.00	7.83
Pmmm KB_{10}	50	0.44	625.06	6.06	4.33
o-B_{15}	0	0.75	392.41	19.54	15.86
o-B_{14}	0	0.83	582.84	18.73	29.12
o-B_{36}	0	0.84	538.89	17.93	28.11
o-B_{10}	0	0.79	483.55	7.56	22.19

Table S7. Superconducting properties of B allotropes.

Structure	low-frequency(%)	middle-frequency(%)	high-frequency(%)
o-B_{15}	53.18 (0–470 cm^{-1})	45.02 (470–1000 cm^{-1})	1.89 (>1000 cm^{-1})
o-B_{14}	60.90 (0–450 cm^{-1})	35.57 (450–1080 cm^{-1})	3.53 (>1080 cm^{-1})
o-B_{36}	54.75 (0–390 cm^{-1})	41.44 (390–900 cm^{-1})	3.81 (>900 cm^{-1})
o-B_{10}	56.24 (0–370 cm^{-1})	39.68 (370–930 cm^{-1})	4.08 (>930 cm^{-1})

Table. S8 Superconducting properties of metastable K–B structures.

Structure	low-frequency(%)	middle-frequency(%)	high-frequency(%)
*Pmm*2 KB_5	63.60 (0–370 cm^{-1})	34.14 (370–1200 cm^{-1})	2.26 (> 1200 cm^{-1})
Immm KB_9	18.28 (0–300 cm^{-1})	79.88 (300–1150 cm^{-1})	1.84 (> 1150 cm^{-1})
Pmmm KB_{10}	33.11 (0–300 cm^{-1})	65.29 (300–1150 cm^{-1})	1.60 (> 1150 cm^{-1})

References

1. L. Xiao, J. Ran, Y. Liu, J. Wu, W. Qiu, F. Lu, F. Shao and P. Peng, *Comput. Condens. Matter*, 2016, **9**, 1–5.
2. Z. Yuan, L. Hao, K. Luo, M. Xiong, C. Shao, F. Ling and D. Yu, *Chem. Phys. Lett.*, 2019, **722**, 80–84.
3. A. R. Oganov and V. L. Solozhenko, *J. Superhard. Mater.*, 2009, **31**, 285.
4. Z.-j. Wu, E.-j. Zhao, H.-p. Xiang, X.-f. Hao, X.-j. Liu and J. Meng, *Phys. Rev. B*, 2007, **76**, 054115.